Appl. Phys. B 90, 255–262 (2008)
DOI: 10.1007/s00340-007-2842-0

Applied Physics B
Lasers and Optics

K.S. BOND
N.D. COLLETT
E.P. FULLER
J.L. HARDWICK✉
E.E. HINDS
T.W. KEIBER
I.S.G. KELLY-MORGAN
C.M. MATTHYS
M.J. PILKENTON
K.W. SINCLAIR
A.A. TAYLOR

Temperature dependence of pressure broadening and shifts of acetylene at 1550 nm by He, Ne, and Ar

Department of Chemistry, University of Oregon, Eugene, OR 97403, USA

Received: 14 September 2007 /
Revised version: 10 October 2007
Published online: 28 November 2007 • **© Springer-Verlag 2007**

ABSTRACT Pressure broadening and shift coefficients for the $\nu_1 + \nu_3$ band of $^{12}C_2H_2$ have been measured for He, Ne, and Ar at a temperature of 195 K using high resolution diode laser spectroscopy. The pressure broadening and shifts follow patterns with rotational assignment that are similar to those at room temperature but are generally larger in magnitude. The change in magnitude is qualitatively described by assuming, for each transition, a constant cross section for pressure broadening or shifting. Better agreement may be obtained for pressure broadening coefficients by using empirically determined temperature exponents; better agreement still is obtained from close coupling calculations of the pressure broadening cross sections.

PACS 33.70.Jg

1 Introduction

1.1 *Background*

The development over the past two decades of tunable diode lasers in the near and mid-infrared has allowed molecular spectroscopy of small molecules in the gas phase with an instrumental resolution several orders of magnitude narrower than typical molecular line widths. Consequently, the shapes of molecular absorption lines may now be examined with far greater accuracy than has heretofore been possible. Acetylene in particular has attracted a great deal of recent interest in the pressure dependence of line shapes; this interest arises due to both the importance of acetylene in atmospheric and combustion chemistry and to its usefulness as a prototype for modeling pressure-dependent line shape [1–37].

The study of pressure broadening and shifts of molecular absorption lines is important for both fundamental and practical reasons. From a fundamental perspective, the broadening and shifts of transitions due to collisions are experimental consequences of the intermolecular forces between gas molecules. In practical terms, accurate collisional broadening and shift coefficients are essential for analytical purposes such as remote atmospheric sensing.

A recent series of papers by Thibault, Cappelletti, and coworkers [1–4] has presented calculations of pressure broadening coefficients of acetylene by the rare gases using either ab initio or semi-empirical potential functions, comparing those calculations with the available experimental work.

A recent paper from this laboratory [5] reported measurements of the pressure broadening coefficients of the $\nu_1 + \nu_3$ band of acetylene by several buffer gases at room temperature; these were found to be in good agreement with the calculated values of Thibault et al. This paper extends those measurements to −78 °C for the buffer gases helium, neon, and argon.

1.2 *Line shape function*

Consistent with our previous paper, the Voigt profile is used to model the shape of the acetylene absorption lines. The Voigt profile, a convolution of a Gaussian and a Lorentzian line shape, is approximated in this work using the algorithm due to Humlicek [38], which has been demonstrated to reproduce the Voigt function with an error of 1 part in 10^4 or less. The Voigt function does not include such phenomena as Dicke narrowing [39] and the differential efficiency of collisional broadening as a function of the translational energy of the collision [13]. The difference between the Voigt profile and a more sophisticated model appears, however, to be below the noise level of the present experiment, thus the Voigt function is used. Also for consistency and ease of comparison with our first paper, the pressure broadening coefficient is quoted in terms of the full width at half maximum (FWHM) of the Lorentzian component of the Voigt profile.

2 Experimental details

2.1 *Equipment*

The details of the experiment are similar to those previously reported [40]. The laser was an external cavity diode laser (New Focus 6428). Part of the laser light was picked off by a mirror and directed through an internally coupled Fabry–Pérot interferometer (FP) with a free spec-

✉ Fax: +1 541 346-4643, E-mail: hardwick@uoregon.edu

tral range of 0.009725 cm^{-1}. Part of the remaining light was picked off using a second mirror. One of the beams was passed through a 1-m reference cell filled with pure acetylene at a pressure of 2 Torr to provide an absolute wavelength calibration. The other part was directed through the sample cell. In each of the three paths, light was detected using an InGaAs detector (ThorLabs PDA400) amplified using a home-built variable-gain preamplifier with variable offset, and recorded using an A/D converter (National Instruments PCI-6221).

The sample cell was a single-pass stainless steel cell with a path length of 1 m, equipped with wedged windows and packed in crushed dry ice. Copper tubing was used to extend the cooling area past the windows in an effort to keep the temperature uniform over the active length of the cell. Dry nitrogen was passed over the windows to prevent icing.

An absolute accuracy of approximately 10 MHz was routinely obtained for unblended lines. The spectral line width of the laser was dominated by a jitter of approximately 0.0003 cm^{-1} over a time scale of about 20 μs.

Acetylene was synthesized from water and calcium carbide and distilled from a low temperature trap into a stainless steel tank for storage. This sample was found to last for several weeks without deterioration. Buffer gases were used with a purity greater than or equal to 99.8%. Pressures were measured using a temperature compensated pressure sensor (SenSym 19C015A4) and were monitored frequently during these experiments to guard against leaks resulting from temperature cycling of the vacuum seals.

The pressure broadening and shift coefficients were measured several times for each buffer gas in order to minimize the effects arising from the slow drift of the baseline. This baseline drift, which was subsequently removed in software, was due to the shifting load on the cell as the dry ice sublimed. This drift proved most troublesome for high buffer gas pressures where the combination of baseline drift, large line width and low peak intensities compromised some data sets to the point that they could not be used.

2.2 *Data collection and analysis*

Data collection was performed with Igor Pro 5 (WaveMetrics, Inc.), using Igor NIDAQ Tools MX to control the interface card. Data were digitized with 16-bit resolution so that the S/N ratio was not limited by digitizing error. The noise level, which amounts to about 0.1% of the full scale signal in the sample channel, is believed to be due do a combination of laser jitter, accidental étalons, and detector noise. The laser was also controlled with Igor Pro using a GPIB interface.

The laser scanned at a rate of 1 nm/s, the minimum scan speed for this unit. Scanning at this rate, the laser was found to scan reliably from 6450 to 6650 cm^{-1} without mode hops. Data collection was set at 50 000 samples/s, providing a collection resolution of 8×10^{-5} cm^{-1} per data point. The Doppler width of an isolated absorption line of acetylene is 0.012 cm^{-1} at 195 K, so the profile of a single Doppler-broadened line was sampled with approximately 150 data points. There were about 100 points in the free spectral range of the interferometer used for calibration. Laser power was set between 0.5 and 1.0 mW.

2.3 *Method*

During a single experiment, the partial pressure of acetylene remained unchanged at a pressure of about 1 Torr. The pressure of the buffer gas was then increased in intervals of 10 to 50 Torr up to a maximum total pressure of about 0.5 atm. (1 atm = 760 Torr = 101 325 Pa.) In this way, 10 or more spectra could be recorded with differing pressures of the buffer gas and the same partial pressure (and thus the same integrated absorbance) of acetylene. A constant quantity of dry ice was maintained to replace material lost to sublimation.

IgorPro 5 (WaveMetrics, Inc.) was used to calibrate the wavenumber scale of the spectra, convert the raw signal to absorbance, and perform nonlinear fits to all of the spectra at different pressures of buffer gas simultaneously (a "multispectrum" fit [12, 41]). The Doppler width was found from repeated experiments to be indistinguishable from the theoretical value at 195 K, and so the Doppler component of the Voigt profile was held fixed at the theoretical value.

3 Results

3.1 *Observations*

A detail from a typical set of spectra is presented in Fig. 1. The $P(17)$ line in this figure has a typical signal/noise ratio and pressure broadening and shift coefficients. The line clearly illustrates the shift of the line center to a lower wavenumber with a higher pressure.

The spectra observed in this experiment are, on the whole, less cluttered than those observed at room temperature because of the suppression of overlapping hot bands. Accordingly, the pressure broadening and shift coefficients are somewhat less prone to systematic error than those obtained from the higher temperature spectra. The range of quantum num-

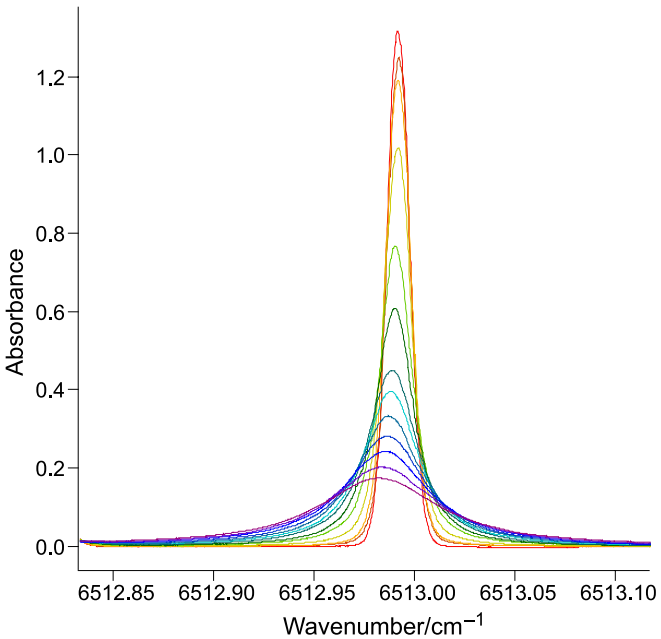

FIGURE 1 A single line of the spectrum of the $\nu_1 + \nu_3$ band of acetylene broadened and shifted by argon at 195 K. The $P(17)$ line is shown with a partial pressure of argon from 0 up to a maximum of 396 Torr. The acetylene pressure is approximately 0.7 Torr

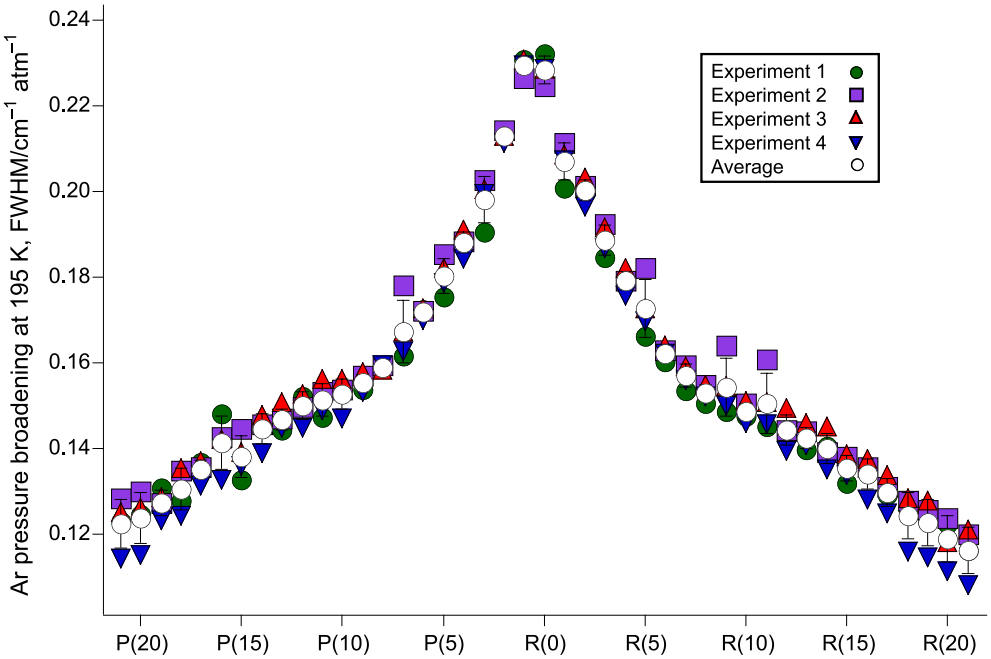

FIGURE 2 Pressure broadening coefficients for broadening of the $\nu_1 + \nu_3$ band of C_2H_2 by Ar at 195 K. The results of four independent experiments are presented

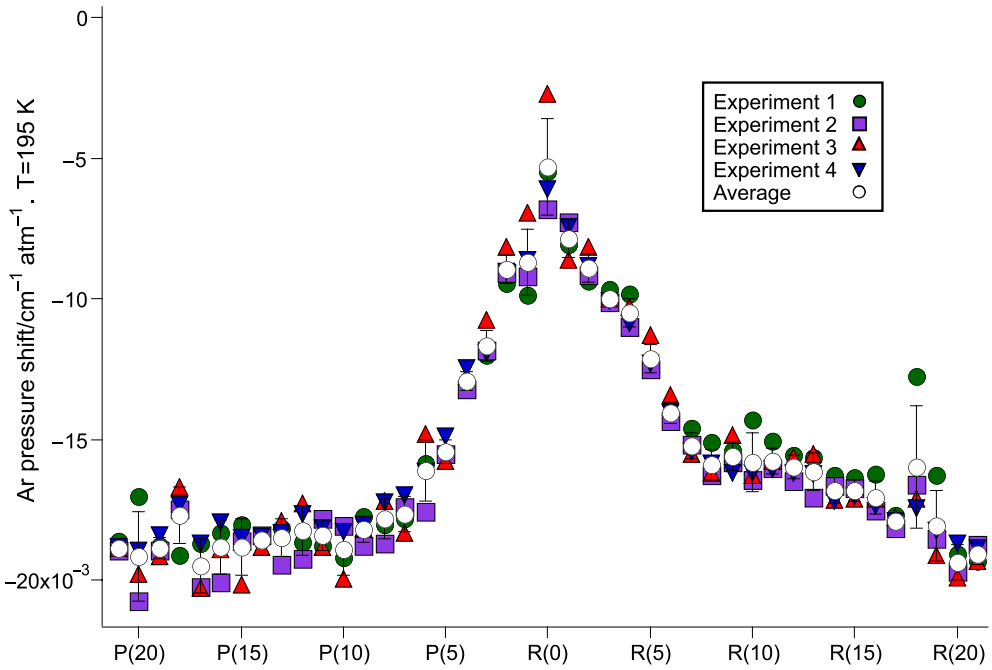

FIGURE 3 Pressure shift coefficients for shifting of the $\nu_1 + \nu_3$ band of C_2H_2 by Ar at 195 K. The results of four independent experiments are presented

bers is, however, more restricted, owing to the depopulation of high-J states at lower temperature.

Pressure broadening coefficients (FWHM) for argon from four independent sequences of spectra are presented in Fig. 2. These coefficients exhibit a scatter somewhat greater than what would be expected based on the standard deviation of the fits, indicating that their average will absorb some of the systematic errors introduced from any particular experiment. The corresponding pressure shift coefficients are presented in Fig. 3. The open circles represent the averages of the experimental values. Error bars in Figs. 2 and 3 are one standard deviation.

The pressure broadening coefficients obtained for He, Ne, and Ar are presented in Table 1, and the pressure shift coefficients are presented in Table 2. Estimated uncertainties are one standard deviation.

3.2 *Temperature scaling of pressure broadening*

As expected, both the pressure broadening and pressure shift coefficients are significantly larger at 195 K than at 295 K. In the simplest approximation, the pressure broadening and shift coefficients are determined by a collisional cross section that is independent of temperature. At constant pressure, the density of gas varies inversely with temperature and the RMS velocity varies as the square root of temperature. Therefore, this simple approximation predicts that the pressure broadening and pressure shift coefficients

Line	He	He (calc)	Ne	Ne (calc)	Ar
$P(21)$	0.1027(42)	0.1026	0.0796(42)	0.0796	0.1227(56)
$P(20)$	0.1048(57)		0.0801(46)	0.0819	0.1240(59)
$P(19)$	0.1041(30)		0.0837(55)	0.0842	0.1275(29)
$P(18)$	0.1025(80)		0.0825(32)	0.0866	0.1306(50)
$P(17)$	0.1049(32)		0.0873(15)	0.0885	0.1352(22)
$P(16)$	0.1050(44)		0.0893(31)	0.0904	0.1414(62)
$P(15)$	0.1041(43)		0.0890(21)	0.0922	0.1382(50)
$P(14)$	0.1042(32)		0.0925(28)	0.0936	0.1446(35)
$P(13)$	0.1047(28)		0.0934(27)	0.0946	0.1468(25)
$P(12)$	0.1050(34)		0.0945(38)	0.0954	0.1500(31)
$P(11)$	0.1037(33)	0.1060	0.0961(25)	0.0956	0.1514(37)
$P(10)$	0.1030(46)		0.0956(44)	0.0970	0.1528(34)
$P(9)$	0.1024(26)		0.0965(35)	0.0974	0.1556(18)
$P(8)$	0.1015(36)		0.0963(73)	0.0978	0.1590(11)
$P(7)$	0.1015(41)		0.0992(37)	0.0994	0.1675(74)
$P(6)$	0.1002(43)		0.1053(34)	0.1020	0.1719(8)
$P(5)$	0.1025(27)		0.1090(21)	0.1070	0.1805(42)
$P(4)$	0.1010(43)		0.1134(76)	0.1120	0.1882(24)
$P(3)$	0.1041(53)		0.1192(58)	0.1180	0.1983(53)
$P(2)$	0.1080(42)		0.1248(72)	0.1240	0.2129(11)
$P(1)$	0.1214(42)	0.1258	0.1377(113)	0.1360	0.2295(19)
$R(0)$	0.1185(44)	0.1258	0.1407(125)	0.1360	0.2285(32)
$R(1)$	0.1068(44)		0.1267(51)	0.1240	0.2070(44)
$R(2)$	0.1041(40)		0.1169(97)	0.1180	0.2003(24)
$R(3)$	0.1017(43)		0.1145(31)	0.1120	0.1889(35)
$R(4)$	0.1009(35)		0.1092(38)	0.1070	0.1793(21)
$R(5)$	0.1013(31)		0.1040(36)	0.1020	0.1727(67)
$R(6)$	0.1012(32)		0.1002(37)	0.0994	0.1624(13)
$R(7)$	0.1025(33)		0.0986(26)	0.0978	0.1570(26)
$R(8)$	0.1024(33)		0.0964(47)	0.0974	0.1531(19)
$R(9)$	0.1033(29)		0.0963(32)	0.0970	0.1544(69)
$R(10)$	0.1028(49)	0.1060	0.0939(53)	0.0956	0.1487(20)
$R(11)$	0.1047(34)		0.0944(28)	0.0954	0.1507(71)
$R(12)$	0.1033(39)		0.0911(47)	0.0946	0.1444(34)
$R(13)$	0.1042(39)		0.0921(26)	0.0936	0.1427(25)
$R(14)$	0.1033(50)		0.0907(26)	0.0922	0.1400(35)
$R(15)$	0.1046(39)		0.0899(14)	0.0904	0.1356(30)
$R(16)$	0.1034(48)		0.0856(32)	0.0885	0.1342(36)
$R(17)$	0.1024(47)		0.0853(15)	0.0866	0.1297(32)
$R(18)$	0.1008(44)		0.0798(48)	0.0842	0.1245(54)
$R(19)$	0.1018(56)		0.0810(21)	0.0819	0.1228(54)
$R(20)$	0.1000(49)	0.1026	0.0792(69)	0.0796	0.1190(54)
$R(21)$	0.1012(49)		0.0780(50)		0.1163(54)

TABLE 1 Pressure broadening coefficients for broadening of the $\nu_1 + \nu_3$ band of C_2H_2 by He, Ne, and Ar at 195 K. Units are cm^{-1}/atm. The coefficient quoted here is the contribution to the full width at half maximum of the Lorentz component of the Voigt function. Values were averaged from four independent experiments in the case of argon and five for helium and neon. Each experiment consisted of a minimum of 10 spectra with a range of buffer gas pressures from 0 to 400 Torr. Errors of one standard deviation are given in parentheses in units of the least significant figure of the coefficient. The calculated values for helium and neon are due to Thibault [1, 3, 43]

will scale as $T^{-1/2}$. While there are usually deviations from this simple scaling law, it is common to represent the scaling as T^{-n}, where n usually tends toward the classical limit of 0.5 in the limit of high T and high rotational quantum number [3]. Temperature scaling has been explored, in the case of acetylene pressurized by the rare gases, for the pressure broadening coefficients [1–3, 7, 8, 10, 13, 28]; the corresponding scaling laws for pressure shift have not been well investigated.

3.2.1 Neon. Thibault and co-workers [3] have recently published an experimental and theoretical investigation of the pressure broadening and scattering cross sections of acetylene by neon. Their theoretical treatment compared two potential energy functions used to describe the collision: a parameterized potential function based on an atom-bond model and a symmetry adapted perturbation theory (SAPT) ab initio potential function due to Bemish and co-workers [42]. Of the two, the SAPT potential was particularly good at reproducing the experimental pressure broadening coefficients at 298 K and 173 K. Thibault [43] has provided us with additional calculations based on the SAPT potential for a temperature of 195 K which are displayed in Fig. 4. As can be seen, the experiment and theory are in excellent agreement: the prediction falls within our experimental uncertainty in all cases.

For comparison, we have also computed the pressure broadening coefficients for 195 K predicted from the relation

$$\gamma_0^{195\ \mathrm{K}} = \gamma_0^{173\ \mathrm{K}} \left(\frac{173}{195}\right)^n , \tag{1}$$

where $\gamma_0^{(T)}$ represents the pressure broadening coefficient at a particular temperature T. Both $\gamma_0^{173\ \mathrm{K}}$ and n have been taken from Table 1 of Thibault et al. [3], who use the convention of half width at half maximum to describe the pressure broadening coefficient. The prediction based on this simpler scaling law shows similar good agreement with the present experiment.

3.2.2 Helium. The experimental pressure broadening coefficients for helium are illustrated in Fig. 5. The solid line represents a temperature scaling of the pressure broadening coefficients calculated by Thibault [1]: first, the temperature exponent n was determined using the relationship

Line	He	Ne	Ar
$P(21)$	0.0000(4)	–0.0037(5)	–0.0188(2)
$P(20)$	–0.0003(3)	–0.0044(12)	–0.0191(16)
$P(19)$	–0.0001(1)	–0.0046(8)	–0.0188(4)
$P(18)$	0.0018(9)	–0.0040(11)	–0.0177(10)
$P(17)$	0.0001(2)	–0.0044(5)	–0.0195(10)
$P(16)$	–0.0007(2)	–0.0046(5)	–0.0188(10)
$P(15)$	–0.0002(1)	–0.0055(3)	–0.0188(10)
$P(14)$	–0.0004(3)	–0.0052(6)	–0.0186(3)
$P(13)$	–0.0007(1)	–0.0055(4)	–0.0185(7)
$P(12)$	–0.0006(1)	–0.0058(3)	–0.0182(9)
$P(11)$	–0.0005(2)	–0.0062(5)	–0.0184(5)
$P(10)$	–0.0009(1)	–0.0067(3)	–0.0189(9)
$P(9)$	–0.0007(1)	–0.0063(5)	–0.0182(4)
$P(8)$	–0.0006(1)	–0.0062(3)	–0.0178(7)
$P(7)$	–0.0008(1)	–0.0062(6)	–0.0176(6)
$P(6)$	–0.0007(2)	–0.0062(5)	–0.0161(11)
$P(5)$	–0.0011(1)	–0.0061(3)	–0.0154(4)
$P(4)$	–0.0007(2)	–0.0056(3)	–0.0129(4)
$P(3)$	–0.0011(2)	–0.0047(5)	–0.0116(5)
$P(2)$	–0.0012(4)	–0.0028(4)	–0.0089(5)
$P(1)$	–0.0012(5)	–0.0042(8)	–0.0087(12)
$R(0)$	–0.0012(3)	–0.0043(6)	–0.0053(17)
$R(1)$	–0.0013(1)	–0.0052(5)	–0.0079(7)
$R(2)$	–0.0011(3)	–0.0051(3)	–0.0089(5)
$R(3)$	–0.0009(1)	–0.0051(1)	–0.0100(2)
$R(4)$	–0.0009(1)	–0.0049(4)	–0.0105(5)
$R(5)$	–0.0007(1)	–0.0050(3)	–0.0121(5)
$R(6)$	–0.0007(1)	–0.0050(2)	–0.0141(4)
$R(7)$	–0.0003(3)	–0.0052(16)	–0.0152(4)
$R(8)$	–0.0005(2)	–0.0049(3)	–0.0159(6)
$R(9)$	–0.0004(1)	–0.0048(2)	–0.0156(5)
$R(10)$	–0.0004(1)	–0.0047(4)	–0.0158(10)
$R(11)$	0.0000(1)	–0.0043(3)	–0.0157(5)
$R(12)$	0.0001(1)	–0.0044(3)	–0.0160(4)
$R(13)$	0.0001(1)	–0.0040(2)	–0.0161(7)
$R(14)$	0.0001(1)	–0.0043(3)	–0.0168(5)
$R(15)$	0.0003(2)	–0.0041(2)	–0.0168(4)
$R(16)$	0.0003(4)	–0.0031(5)	–0.0171(6)
$R(17)$	0.0005(2)	–0.0037(3)	–0.0179(2)
$R(18)$	0.0015(6)	–0.0037(23)	–0.0160(22)
$R(19)$	0.0009(1)	–0.0034(3)	–0.0180(13)
$R(20)$	0.0009(6)	–0.0035(12)	–0.0194(6)
$R(21)$	0.0005(1)	–0.0033(3)	–0.0191(4)

TABLE 2 Pressure shift coefficients for shifting of the $\nu_1 + \nu_3$ band of C_2H_2 by He, Ne, and Ar at 195 K. Units are cm^{-1}/atm. Values were averaged from four independent experiments in the case of argon and five for helium and neon. Each experiment consisted of a minimum of 10 spectra with a range of buffer gas pressures from 0 to 400 Torr. Errors of one standard deviation are given in parentheses in units of the least significant figure of the coefficient

$$\gamma_0^{(298\ \mathrm{K})} = \gamma_0^{(173\ \mathrm{K})} \left(\frac{173}{298}\right)^n . \qquad (2)$$

Following this, the pressure broadening coefficients $\gamma_0^{(195\ \mathrm{K})}$ were constructed using (1). The open upward-pointing triangles represent unpublished calculations of Thibault [43]. The molecular scattering calculations were performed in the same way as [1], except that the kinetic energy of the collision was set at 177 cm^{-1}, corresponding to $4kT/\pi hc$ at a temperature of 200 K. The resulting pressure broadening coefficient was scaled from 200 K to 195 K using a temperature exponent $n = 0.44$ (a correction of about 1%).

Both the temperature-scaled coefficients and the coefficients derived from molecular scattering calculations at 177 cm^{-1} are slightly high, though in most cases the difference is not statistically significant. The temperature-scaled

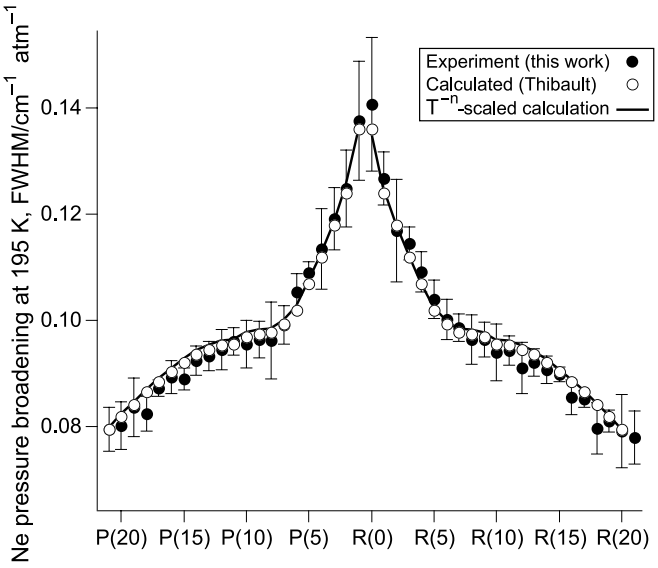

FIGURE 4 Experimental and theoretical pressure broadening coefficients for the broadening of the $\nu_1 + \nu_3$ band of C_2H_2 by Ne at 195 K. *Solid circles* represent experimental coefficients from Table 1; *error bars* are one standard deviation. *Open circles* plot the theoretical coefficients calculated by Thibault [3, 43] using the ab initio potential surface of Bemish et al. [42]. The *solid line* plots the temperature-scaled coefficients of [3] as described in the text

coefficients are higher than the experimental values by an amount ranging from 1% up to about 7%, a discrepancy barely above our experimental uncertainty. The more rigorously calculated pressure broadening coefficients follow the temperature scaling at low J and approach the experimental values closely at high J. The trend of the differences is similar to our previous results at room temperature [5], which are reproduced in Fig. 5 for comparison.

3.2.3 Argon. The pressure broadening coefficients are largest for argon of the three buffer gases studied here, owing to the depth of the intermolecular potential between argon and acetylene. While this makes the pressure broadening coefficients easier to observe experimentally, it makes them more difficult to calculate theoretically and more problematic to scale with temperature.

Pressure broadening coefficients for argon at 195 K are displayed in Fig. 6. Theoretical pressure broadening coefficients for 297 K and 173 K have been reported by Cappelletti et al. [2], and the coefficients at 173 K have been scaled to 195 K by (1) and (2) using the method described above for helium broadening. The scaled coefficients are in good agreement with experiment except for the transitions involving the lowest rotational quantum numbers. We regard this divergence at low rotational quantum number as resulting from the simplicity of our scaling technique rather than the quality of the theoretical calculations.

3.3 *Temperature scaling of pressure shifts*

Pressure shifts have received far less attention than pressure broadening for several reasons. First, the small shifts of the line centroids are difficult to measure

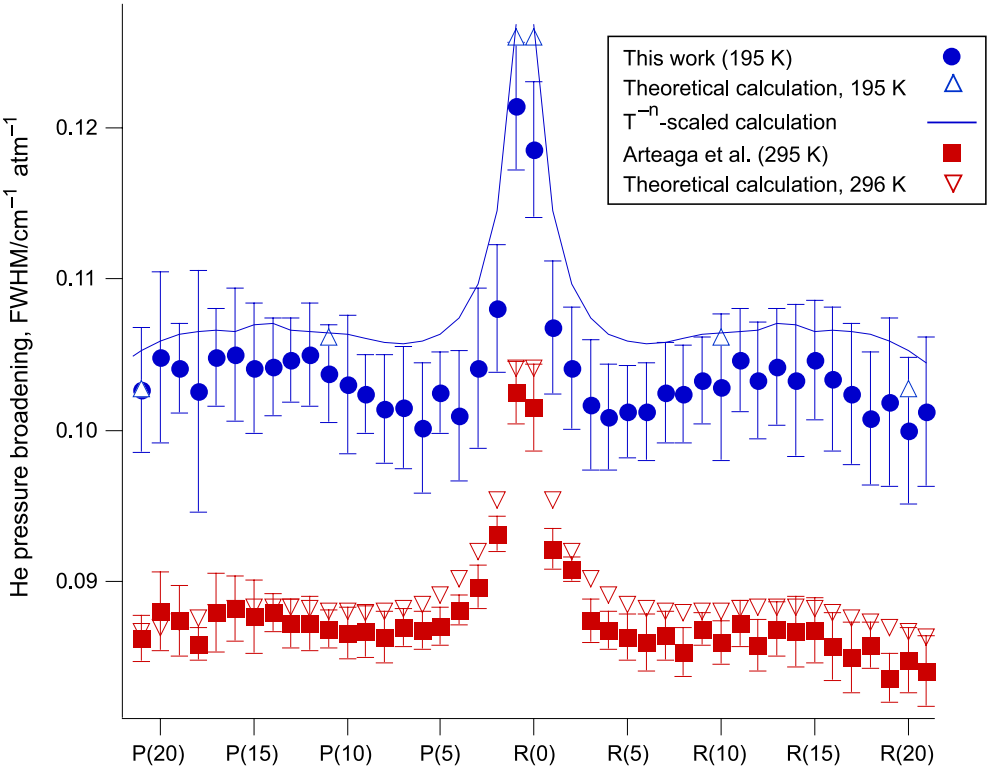

FIGURE 5 Experimental and theoretical pressure broadening coefficients for the broadening of the $\nu_1 + \nu_3$ band of C_2H_2 by He at 295 and 195 K. *Solid circles* represent experimental coefficients from Table 1; *error bars* are one standard deviation. The *solid line* plots the temperature-scaled coefficients of [1] as described in the text. Data at 295 K are from Arteaga et al. [5]

under the best of circumstances, requiring both high resolution and high reproducibility of the wavenumber scale. Moreover, the pressure shift coefficients, unlike pressure broadening coefficients, depend quite strongly on the vibrational transition under investigation; accordingly, it is not productive to compare pressure shift coefficients at different temperatures unless the vibrational transition is the same.

Finally, pressure shift coefficients are difficult to model, depending on not only the vibrational and rotational quantum numbers but also on the (vibrationally-dependent) average trajectory of the collision [44, 45]. Accordingly, an accurate vibrationally-dependent intermolecular potential energy surface is required for the calculation, and these are not readily available in most cases. The shifts are sensitive to the details of the intermolecular potential, and, while this provides addi-

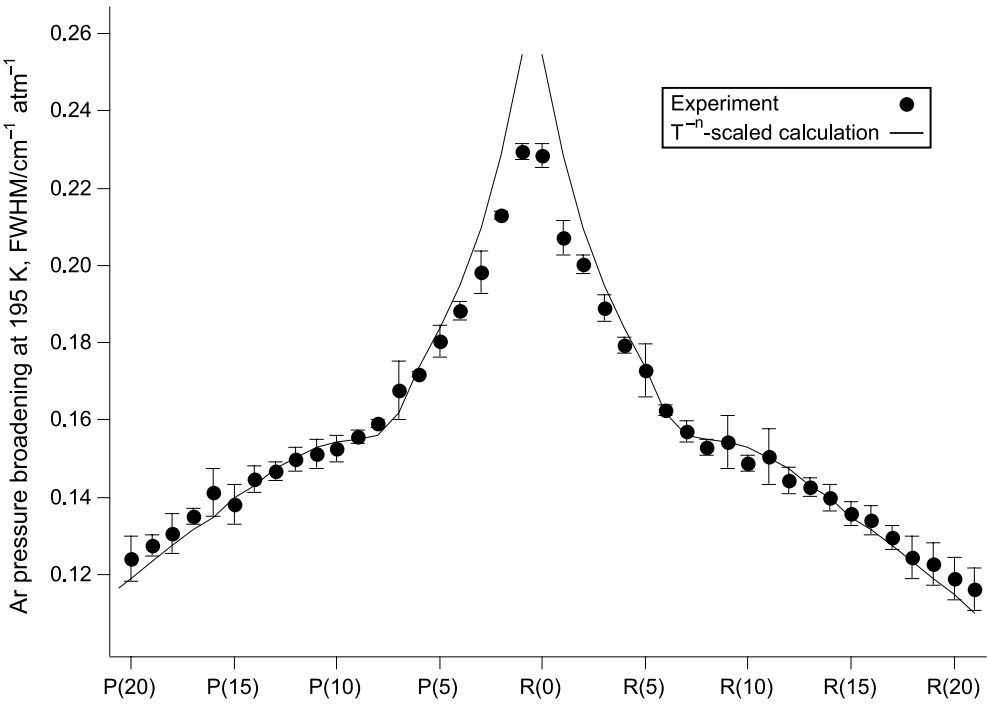

FIGURE 6 Experimental and temperature-scaled pressure broadening coefficients for the shift of the $\nu_1 + \nu_3$ band of C_2H_2 by Ar at 195 K. *Solid circles* represent experimental coefficients from Table 1; *error bars* are one standard deviation. The *solid line* plots the temperature-scaled coefficients of [2] as described in the text

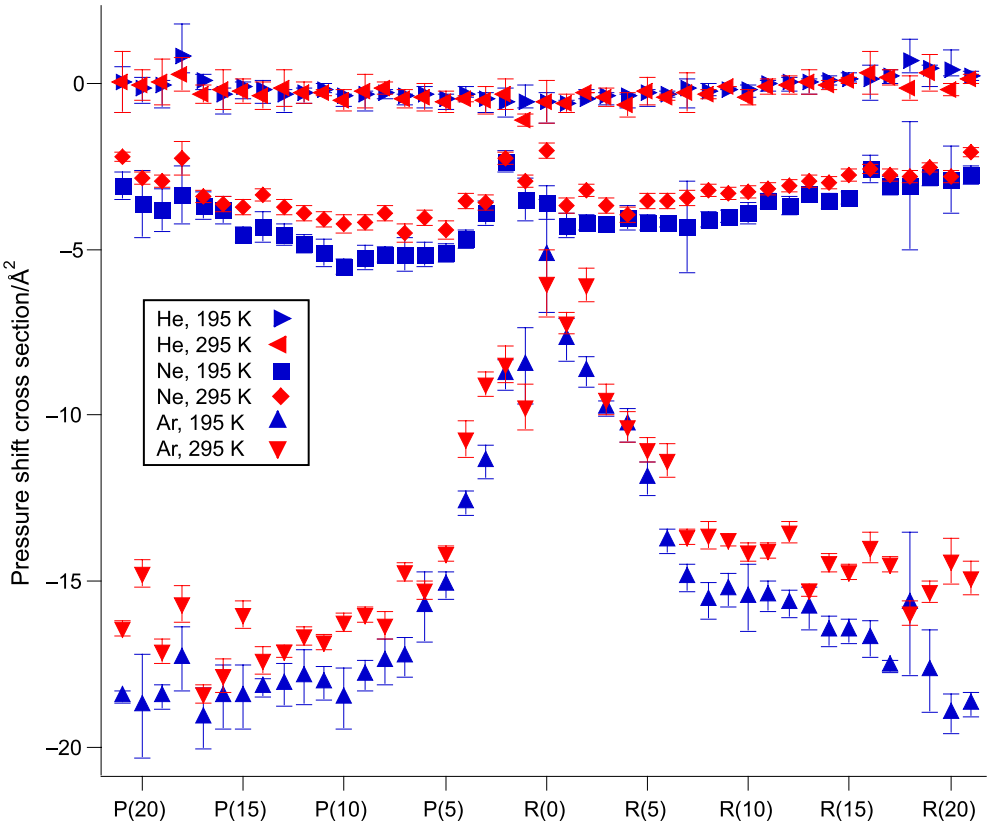

FIGURE 7 Pressure shift cross sections for the $\nu_1 + \nu_3$ band of acetylene at 195 K (present work) and 295 K (Arteaga et al. [5]). *Error bars* are one standard deviation

tional information on the potential function, the information is not trivial to extract [44]. Foley, in his seminal paper on collisional broadening and shifts, estimated the ratio of the pressure shift coefficient to the pressure broadening coefficient based on the leading term in the long-range force dominating the collision [46]. For vibrational transitions, these estimates are not useful: they are able to predict neither the order of magnitude nor the sign of the pressure shift coefficient from the pressure broadening coefficient. It is our hope that the experimental data presented here will help guide a more accurate theoretical approach to this problem.

Taking the pressure shift coefficients at 195 K from Table 2 and the corresponding coefficients at 295 K from Table 2 of Arteaga et al. [5], we are able to compute the pressure shift cross sections for the present band of acetylene at both 195 K and 295 K for He, Ne, and Ar. Writing the change in angular frequency $\delta\omega$ in terms of the cross section σ_S, the density of collision partners N, and the RMS velocity $\bar{v}$ as $\delta\omega = N\bar{v}\sigma_S$, we obtain the pressure shift coefficient δ_0 in terms of wavenumber per unit pressure as

$$\delta_0 = \frac{1}{2\pi c k_B T}\bar{v}\sigma_S \,. \tag{3}$$

Equation (3) is algebraically equivalent to Thibault's (1) in [1], although the physical meaning of the cross section is different. In particular, the pressure shift cross section σ_S may assume either positive or negative values, while the pressure broadening cross section is always positive.

These pressure shift cross sections are compared in Fig. 7. While the cross sections are significantly different at 195 K and 295 K, the difference is not great, and a simple linear interpolation will probably be adequate to predict the pressure shift cross section at any intermediate temperature.

4 Discussion

As expected, the $P(J)$ and $R(J-1)$ lines are found to have identical pressure broadening coefficients within our experimental uncertainty, indicating that the vibrationally-dependent contribution to the pressure broadening is small. In contrast, the pressure shift has a noticeably asymmetric distribution; the utility of this asymmetry in probing the intermolecular potential has been pointed out by Luo et al. [44]. Since the temperature dependence deviates significantly from $T^{-1/2}$ for both the pressure broadening and the pressure shift coefficients, the assumption of a cross section that is constant with temperature is only moderately useful. For the pressure broadening cross section, an empirical law of the form T^{-n} gives good results in the investigated temperature range and is simple to use, and it appears that n can reliably be predicted from theoretical calculations, at least for pressure broadening coefficients. Scattering calculations based on ab initio potential functions are shown to be quite good at predicting broadening coefficients, though they are considerably more difficult in practice than the simple T^{-n} scaling function. In particular, the noticeable "kinks" in the pressure broadening coefficients between $J = 5$ and 10 are well-reproduced by theory, as illustrated in Figs. 4–6.

5 Conclusion

Pressure broadening and pressure shift coefficients have been measured at 195 K for the $\nu_1 + \nu_3$ band of acetylene

using a tunable diode laser spectrometer. Where comparisons are possible, the measured pressure broadening coefficients are in excellent agreement with theoretical calculations. The results are also in good agreement with temperature-scaled measurements of theoretical pressure broadening coefficients at 298 K and 173 K. The pressure shift coefficients have been compared with those obtained previously for the same band at room temperature. The pressure shift, as expected, is greater in magnitude at low temperature, although it deviates somewhat from a simple $T^{-1/2}$ power law.

ACKNOWLEDGEMENTS The authors are grateful to Franck Thibault for sharing the results of his calculation of the pressure broadening of acetylene by neon and helium at 195 K. This work was a class project of the Physical Chemistry Laboratory at the University of Oregon. The authors are grateful to the University of Oregon and the Department of Chemistry Instructional Laboratories for their support.

REFERENCES

1 F. Thibault, J. Mol. Spectrosc. **234**, 286 (2005)
2 D. Cappelletti, M. Bartolomei, M. Sabido, F. Pirani, G. Blanquet, J. Walrand, J.-P. Bouanich, F. Thibault, J. Phys. Chem. A **109**, 8471 (2005)
3 F. Thibault, D. Cappelletti, F. Pirani, G. Blanquet, M. Bartolomei, Eur. Phys. J. D **44**, 337 (2007)
4 D. Cappelletti, M. Bartolomei, E. Carmona-Novillo, F. Pirani, G. Blanquet, F. Thibault, J. Chem. Phys. **126**, 064 311 (2007)
5 S.W. Arteaga, C.M. Bejger, J.L. Gerecke, J.L. Hardwick, Z.T. Martin, J. Mayo, E.A. McIlhattan, J.M.F. Moreau, M.J. Pilkenton, M.J. Polston, B.T. Robertson, E.N. Wolf, J. Mol. Spectrosc. **243**, 253 (2007)
6 B. Martin, J. Walrand, G. Blanquet, J.-P. Bouanich, M. Lepere, J. Mol. Spectrosc. **236**, 52 (2006)
7 S.V. Ivanov, L. Nguyen, J. Buldyreva, J. Mol. Spectrosc. **233**, 60 (2005)
8 J. Buldyreva, S.V. Ivanov, L. Nguyen, J. Raman Spectrosc. **36**, 148 (2005)
9 J. Buldyreva, L. Nguyen, Mol. Phys. **102**, 1523 (2004)
10 J.L. Domenech, F. Thibault, D. Bermejo, J.-P. Bouanich, J. Mol. Spectrosc. **225**, 48 (2004)
11 D. Jacquemart, J.Y. Mandin, V. Dana, L. Regalia-Jarlot, J. Plateaux, D. Decatoire, L.S. Rothman, J. Quant. Spectrosc. Radiat. Transf. **76**, 237 (2003)
12 D. Jacquemart, J.Y. Mandin, V. Dana, L. Regalia-Jarlot, X. Thomas, P. Von der Heyden, J. Quant. Spectrosc. Radiat. Transf. **75**, 397 (2002)
13 J.-P. Bouanich, J. Walrand, G. Blanquet, J. Mol. Spectrosc. **219**, 98 (2003)
14 J.-P. Bouanich, J. Walrand, G. Blanquet, J. Mol. Spectrosc. **216**, 266 (2002)
15 J.-P. Bouanich, D. Lambot, G. Blanquet, J. Walrand, J. Mol. Spectrosc. **140**, 195 (1990)
16 J.-P. Bouanich, C. Boulet, G. Blanquet, J. Walrand, D. Lambot, J. Quant. Spectrosc. Radiat. Transf. **46**, 317 (1991)
17 J.-P. Bouanich, G. Blanquet, J. Walrand, J. Mol. Spectrosc. **203**, 41 (2000)
18 J.-P. Bouanich, G. Blanquet, J. Walrand, J. Mol. Spectrosc. **194**, 269 (1999)
19 J.-P. Bouanich, G. Blanquet, J.C. Populaire, J. Walrand, J. Mol. Spectrosc. **190**, 7 (1998)
20 C. Yelleswarapu, A. Sharma, J. Quant. Spectrosc. Radiat. Transf. **72**, 733 (2002)
21 C. Yelleswarapu, A. Sharma, J. Quant. Spectrosc. Radiat. Transf. **69**, 151 (2001)
22 M. Thompson, J.G. Baker, N.J. Bowring, J. Mol. Spectrosc. **216**, 24 (2002)
23 H. Valipour, D. Zimmermann, J. Chem. Phys. **114**, 3535 (2001)
24 P. Minutolo, C. Corsi, F. D'Amato, M. De Rosa, Eur. Phys. J. D **17**, 175 (2001)
25 M. Kusaba, J. Henningsen, J. Mol. Spectrosc. **209**, 216 (2001)
26 B.K. Dutta, D. Biswas, B. Ray, P.N. Ghosh, Eur. Phys. J. D **13**, 337 (2001)
27 B.K. Dutta, D. Biswas, B. Ray, P.N. Ghosh, Eur. Phys. J. D **11**, 99 (2000)
28 G. Blanquet, J. Walrand, J.-P. Bouanich, J. Mol. Spectrosc. **210**, 1 (2001)
29 W.C. Swann, S.L. Gilbert, J. Opt. Soc. Am. B **17**, 1263 (2000)
30 F. Herregodts, D. Hurtmans, J. Vander Auwera, M. Herman, Chem. Phys. Lett. **316**, 460 (2000)
31 F. Herregodts, D. Hurtmans, J. Vander Auwera, M. Herman, J. Chem. Phys. **111**, 7954 (1999)
32 F. Herregodts, M. Hepp, D. Hurtmans, J. Vander Auwera, M. Herman, J. Chem. Phys. **111**, 7961 (1999)
33 J. Bood, P.E. Bengtsson, M. Alden, Appl. Phys. B **70**, 607 (2000)
34 B. Lance, G. Blanquet, J. Walrand, J.C. Populaire, J.-P. Bouanich, D. Robert, J. Mol. Spectrosc. **197**, 32 (1999)
35 D. Biswas, B. Ray, S. Dutta, P.N. Ghosh, Appl. Phys. B **68**, 1125 (1999)
36 A. Babay, M. Ibrahimi, V. Lemaire, B. Lemoine, F. Rohart, J.-P. Bouanich, J. Quant. Spectrosc. Radiat. Transf. **59**, 195 (1998)
37 R. Georges, D. van der Vorst, M. Herman, D. Hurtmans, J. Mol. Spectrosc. **185**, 187 (1997)
38 J. Humlicek, J. Quant. Spectrosc. Radiat. Transf. **21**, 309 (1979)
39 R. Dicke, Phys. Rev. **89**, 472 (1953)
40 J.L. Hardwick, Z.T. Martin, E.A. Schoene, V. Tyng, E.N. Wolf, J. Mol. Spectrosc. **239**, 208 (2006)
41 D.C. Benner, C.P. Rinsland, V.M. Devi, M.A.H. Smith, D. Atkins, J. Quant. Spectrosc. Radiat. Transf. **53**, 705 (1995)
42 R.J. Bemish, L. Oudejans, R.E. Miller, R. Moszynski, T.G.A. Heijmen, T. Korona, P.E.S. Wormer, A. van der Avoird, J. Chem. Phys. **109**, 8968 (1998)
43 F. Thibault, private communication (2007)
44 C. Luo, R. Wehr, J.R. Drummond, A.D. May, F. Thibault, J. Boissoles, J.M. Launay, C. Boulet, J.-P. Bouanich, J.-M. Hartmann, J. Chem. Phys. **115**, 2198 (2001)
45 Q. Ma, R.H. Tipping, C. Boulet, F. Thibault, J. Bonamy, J. Mol. Spectrosc. **243**, 105 (2007)
46 H.M. Foley, Phys. Rev. **69**, 616 (1946)

Copyright of Applied Physics B: Lasers & Optics is the property of Springer Science & Business Media B.V. and its content may not be copied or emailed to multiple sites or posted to a listserv without the copyright holder's express written permission. However, users may print, download, or email articles for individual use.